Axial Dispersion in Liquid Flow Through Packed Beds

STEVEN F. MILLER and C. JUDSON KING

University of California, Berkeley, California

Step-function injection and purging of a dilute salt tracer in water was used to measure axial dispersion for low Reynolds number liquid flow through beds of uniform sized, random packed glass spheres. The resultant data and those of several previous studies are coordinated and interpreted in terms of Reynolds, Schmidt, and Peclet numbers.

Axial dispersion in laminar liquid flow through beds of solids is important for several engineering applications, including ion exchange and miscible displacement in petroleum reservoirs. The present work concerns experimental measurements of axial dispersion during liquid flow in the range of Reynolds numbers between 0.003 and 40 and interpretation of the results in the light of past studies. The work was undertaken because of the importance of this flow range, because of wide discrepancies in the available data, and because of the lack of an accepted theoretical explanation of dispersion behavior under these conditions.

Many previous studies have been made of axial dispersion during fluid flow through beds of particulate solids. The recent review of Perkins and Johnston (*19*) is particularly comprehensive in reporting and analyzing past work. The results of these various investigations have commonly been interpreted in terms of an axial Peclet number d_pU/E', which may also be defined as d_pU_o/E with no resulting change in magnitude. E and E' are equivalent to effective axial diffusivities if a diffusion model is obeyed.

In the case of liquid flow there is considerable disagreement between the available sets of data relating the axial Peclet number to the Reynolds number of flow. A general feature is an increase in Peclet number as the flow undergoes a transition from laminar toward turbulent flow. In the region of laminar flow ($N_{Re} < 10$) the available data indicate that the Peclet number for liquids becomes relatively insensitive to changes in Reynolds number (*1*, *3*, *6* to *9*, *13*, *16*, *20*, *21*, *24*, *27*). There is, however, no consensus concerning the absolute magnitude of the Peclet number in this region, a fact which is confirmed by recent reviews (*4*, *13*, *19*, *23*). Some of the discrepancies may come from the use of irregular particles which are difficult to characterize and from marked changes in fluid physical properties across a dsplacement front. It has also been suggested that there is an effect of particle size beyond that represented by the Peclet and Reynolds groups (*5*, *6*, *19*).

EFFECT OF SCHMIDT NUMBER

A comparison of past measurements indicates substantial difference in behavior between gas and liquid systems. Jacques, Hennico, Moon, and Vermeulen (*13*) show that the product of Peclet number and voidage (ϵN_{Pe}) in liquid systems has a relatively constant value of 0.8 to 0.9 at values of N_{Re}' [$= N_{Re}/(1 - \epsilon)$] above 1,000. At lower values of N_{Re}' there is a gradual decrease in ϵN_{Pe} until a nearly constant value of 0.2 is found for $N_{Re}' < 20$. McHenry and Wilhelm (*17*) in a study of gas systems also found ϵN_{Pe} to be about 0.8 at $N_{Re}' > 500$. On the other hand as N_{Re}' decreases their results indicate a slight reduction in ϵN_{Pe} around $N_{Re}' = 250$ followed by a return to the original high level of $\epsilon N_{Pe} = 0.8$ at still lower N_{Re}'.

McHenry and Wilhelm noted that a relatively constant Peclet number near 2 was in accord with the hypothesis that complete mixing of the fluid occurred once every particle diameter. Jacques et al. (*13*) have extended this explanation by postulating for high Schmidt numbers a unique transition of ϵN_{Pe} downward with decreasing N_{Re} toward another limiting value characteristic of segregation due to the laminar velocity distribution. By analogy to pressure drop measurements Jacques et al. and Perkins and Johnston (*19*) suggest that the transition occurs over a broad range as the turbulence within the various cells ceases to be strong enough to cause complete mixing and as cells of different sizes change from turbulent to laminar flow. They also suggest that the gas phase Peclet numbers rise again to the upper limiting value of ϵN_{Pe} after following the high Schmidt number curve for a short way, because lateral molecular diffusion in the void spaces compensates for segregation due to laminar flow. Thus below $N_{Re}' = 100$ molecular diffusion would be able to keep individual void spaces well mixed in gaseous systems. ϵN_{Pe} should then be constant at 0.8 to 0.9 for gases down to N_{Re} on the order of 1 (for $N_{Sc} \simeq 1$), where axial molecular diffusion should cause a decrease in ϵN_{Pe}. A decrease in gas phase Peclet number at very low Reynolds numbers is confirmed by the results of Carberry and Bretton (*8*), Sinclair and Potter (*22*), and Blackwell et al. (*4*).

The only obvious basic difference between gas and liquid systems lies in the Schmidt number. The high Schmidt number of liquids should delay the effect of molecular diffusion in causing the mixing of individual void spaces until lower values of N_{Re} and should cause the effect of axial molecular diffusion to be unimportant until N_{Re}' is on the order of $1/N_{Sc}$. A seeming paradox arises in that Jacques et al. and Ebach and White (*9*) found ϵN_{Pe} essentially constant at the lower limiting value

of 0.2 for $0.07 < N_{Re} < 0.8$, where one would expect the effect of molecular diffusion on void-space mixing to have become important.

EFFECT OF PARTICLE SIZE

High Reynolds number data have almost invariably been obtained for beds of larger particle sizes, while smaller particle sizes have been employed at low Reynolds number. Klinkenberg and Sjenitzer (*14*) suggested the use of a packing or inhomogeneity factor λ which reflects differences in the geometric configuration of a bed. The axial Peclet number then becomes $2/\lambda$. The concept has been adopted by several subsequent authors (*4, 6, 19, 20*). Klinkenberg and Sjenitzer report values of λ ranging from 1 to 4 for various conditions, while Perkins and Johnston (*19*) suggest that λ is a function of particle diameter, ranging from 1 for regular packing and large particle size up to 10 for random packing of spheres and a particle diameter of 100 μ. Presumably the high value of λ for smaller particles represents more bridgings between particles and greater variations in local voidages which promote a channeling phenomenon.

It is also possible that a pertinent variable is the ratio of column diameter to particle diameter (d_t/d_p), even for values of this ratio above 20 where one normally expects significant column wall effects to be absent. Tompkins et al. (*25*) report elution band widths for ion exchange at $N_{Re} = 0.06$ with a fixed particle size (40 to 60 mesh) and different column diameters. The results suggest that E varies as the 1/3 power of column diameter, which again could be the result of a channeling effect (*26*). Channeling phenomena could well occur over regions comparable to the apparatus size (d_t), whereas dispersion mechanisms within individual voids should be characterized by particle size (d_p).

Past data are inconclusive concerning an independent effect of d_p or (d_t/d_p) within a given study. Ebach and White (*9*) and Raimondi et al. (*20*) found no discernible effect of particle diameter over a range of 0.1 to 7 mm. On the other hand, the data of Carberry and Bretton (*8*), Liles and Geankoplis (*16*), Stahel and Geankoplis (*23*), Brigham et al. (*6*), and Ampilogov et al. (*1*) indicate that ϵN_{Pe} is altered by changes in d_p at fixed N_{Re}, but there is no consensus regarding the magnitude of the effect, nor does the effect appear to be well ordered.

APPARATUS

A schematic of the apparatus is given in Figure 1. The injection system consisted of two single-pole double-throw microvalves which were operated together. These connected one stream to the column, while the other stream travelled through a variable resistance (in the form of a valve) to a drain. The flip of a single switch caused rapid transposition of the streams.

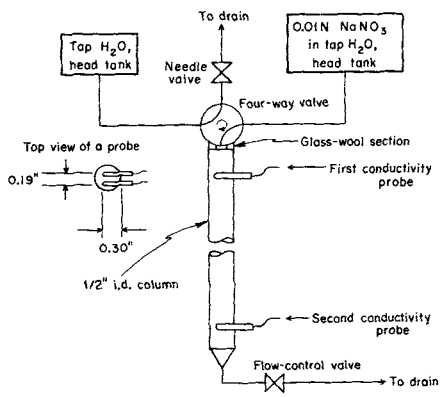

Fig. 1. Schematic of apparatus.

Glass columns, ½ in. I.D. and packed randomly with spheres, were employed for the dispersion studies. Downward flow was employed in the column because earlier experiments indicated a tendency of the bed to fluidize partially even at low N_{Re}'. Alternating runs were carried out with injection (addition of sodium nitrate solution) followed by purging (switching to flow from the tap water tank). In this way it was possible to observe any density or viscosity gradient effect which might influence axial mixing at very low N_{Re}'.

Below the microswitch injection point was a small plug of glass wool followed directly by the first 2 in. of column packing. The first set of electrical conductivity probes was located at this point. The probes consisted of two parallel 1/16-in. rhodium-coated nickel pins 0.30 in. long, lying in a plane perpendicular to the direction of flow. The pins entered the column through a Teflon plug mounted in the wall and were uncapped (but rounded) at their far end. Below the second set of probes was another inch of packing, a screen, and finally a valve which was used to control the flow rate in the column.

Three columns were constructed, differing only in the distance between the two conductivity cells. The lengths of packed bed between cells were 22, 11, and 5½ in. Four sizes of spheres were employed for the measurements. These included 50.8, 99, and 470μ Scotchlite microspheres made by Minnesota Mining and Manufacturing Company. The fourth size was 1.4-mm. glass spheres obtained from Jaymar Scientific, Inc., and donated by Bio-Rad Laboratories of Richmond, California.

EXPERIMENTAL PROCEDURE

The recorder responses for each set of probes were adjusted so that they both yielded readings having the same upper and lower bounds. The chart speed was then set so that the breakthrough curves had close to 45 deg. midpoint slopes, to minimize errors in analysis.

After switching streams, the breakthrough at the upper cell was recorded and then the channels were switched to monitor the breakthrough at the lower cell. This procedure was repeated three more times so that two injections and two purges were recorded. The Peclet numbers for each of the four runs were averaged to give a single datum point.

CALCULATION OF DATA

The analysis of experimental dispersion data has recently been discussed by Klinkenberg (*15*). For large column Peclet numbers (N_{Pe}'), such as those experienced in this study, it becomes impossible to distinguish experimentally between the predictions of most of the models which have been suggested. Peclet numbers were computed from the relationship

$$N_{Pe}' = 4\pi\ S^2 \tag{1}$$

Equation (1) follows the random walk and unbounded diffusion models, among others. Simple division of N_{Pe}' by the ratio of column height to particle diameter yields the packing Peclet number N_{Pe}, which is the quantity of interest.

Since the computation involved the difference in degree of degeneration of a step at two different points in the apparatus, precise measurements were required. The final forms of the equations used to evaluate the experimental data were

$$N_{Pe} = \frac{4\pi\,\epsilon\,d_p}{L}\,\frac{(\Delta h)^2}{\left(\frac{a_2}{\tan\theta_2}\right)^2 - \left(\frac{a_1}{\tan\theta_1}\right)^2} \tag{2}$$

and

$$N_{Re}' = \frac{\epsilon}{1-\epsilon}\,L\,\frac{d_p\,X}{\nu\cdot\Delta h} \tag{3}$$

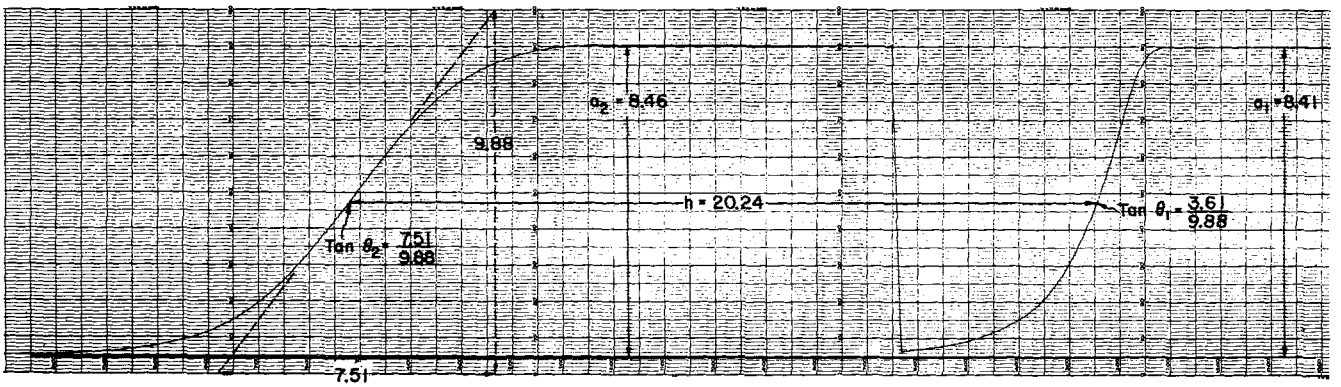

Fig. 2. Typical breakthrough curve. Time proceeds from right to left.

Δh, a_1, $\tan\theta_1$, a_2, and $\tan\theta_2$ were all measured graphically from the breakthrough recordings. Void fractions were measured in a ½-in. I.D. × 2-ft. tubular glass container constructed specifically for that purpose. ϵ was always close to 0.39.

Equation (2) was arrived at in the following manner. For any uniform packing medium Equation (1) indicates that

$$N_{Pe}' = 4\pi\left(\frac{h}{a}\cdot\tan\theta\right)^2 \qquad (4)$$

Since

$$L = (hU/X) \qquad (5)$$

a combination of Equations (4) and (5) with the definition of N_{Pe}' yields

$$\left(\frac{a}{\tan\theta}\right)^2 = 4\pi\ X\cdot\left(\frac{d_p}{U\,N_{Pe}}\right)\cdot h \qquad (6)$$

Since the left-hand side of Equation (6) is linear in h, it is apparent that for the region between any two monitored points in the bed

$$\Delta\left(\frac{a}{\tan\theta}\right)^2 = 4\pi\ X\cdot\left(\frac{d_p}{U\,N_{Pe}}\right)\cdot\Delta h \qquad (7)$$

Furthermore, as long as the response at the two locations is a true degenerate step in shape and the bed is uniform between the two locations, Equation (7) will apply no matter what sort of packing caused the degeneration of the step before the first probe. Equation (7) leads directly to Equation (2).

RESULTS

The response curves did not show a marked amount of asymmetry; the shapes were nearly Gaussian, as predicted by the random walk and unbounded diffusion models at high column Peclet numbers. There was a small amount of tailing, but not in sufficient amount to have any apparent effect on the midpoint slope. On this basis any policy of allowing for the presence of dead spaces in the bed should have no influence on the analysis of the data. Mass balance checks for injection and purging confirmed that the time interval between midpoints agreed within 2% with measured flow rates. A typical breakthrough curve is shown in Figure 2.

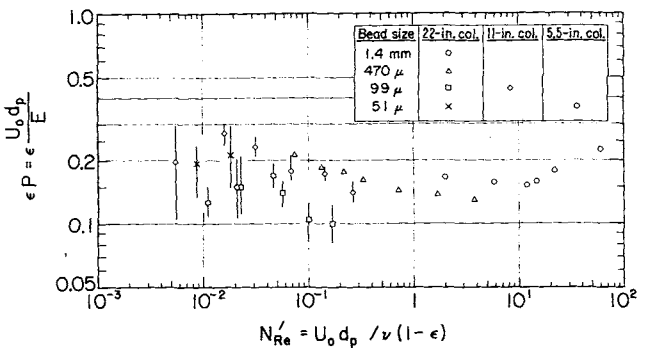

Fig. 3. Experimental results.

The experimental results obtained for different bead sizes and bed lengths are shown in Figure 3. (In the figures N_{Pe} is denoted as P.) A detailed tabulation of the data is available elsewhere (*18*). The brackets associated with each point denote the range of the individual Peclet numbers composing that point. In the cases of the 1.4-mm. and 470-μ glass beads the individual Peclet numbers examined before the averaging process was performed showed very little spread. As bead diameter decreased, the precision also seemed to decrease, especially at very low Reynolds numbers. The entrance section resulted in a fairly constant amount of degeneration in the step function. However, the packed length between cells caused less and less step degeneration as d_p decreased. As a result, the fraction of the total degeneration taking place between probes decreased significantly with d_p so as to affect the precision, but not necessarily the accuracy, of the results.

From the data the following trends were noted:

1. The end of the fall in Peclet number due to the transition from turbulent to laminar flow was observed. Figure 4 demonstrates that the effect observed for the 22-in. column lies between the data of Jacques et al. (*13*) and the data of Ebach and White (*9*), and that all three sets are in acceptable agreement. Frequency response data of Ebach and White for two sphere sizes are included in Figure 4. These are representative of the remainder of their data.

2. As Reynolds number decreases the Peclet number passes through a minimum near $N_{Re}' = 10$ and then rises with a slope of about $-1/6$. The data of Ebach and White also experience a minimum Peclet number in this region and then rise with a similar slope.

3. The limited data below $N_{Re}' = 0.02$ suggest that the Peclet number exhibits a maximum and begins to fall. This fall was echoed in the 50.8-μ data taken in the 22- and 5½-in. columns.

4. Data for 99-μ beads with a 22-in. bed length fall below those for 99-μ beads with an 11-in. bed length. However, data for 50.8-μ beads and a 22-in. bed length fall above those for 50.8-μ beads and a 5½-in. bed length. There is no ordered length effect.

5. Examination of data for 99-, 470-, and 1.4-mm. glass beads reveals no major trend of Peclet number with

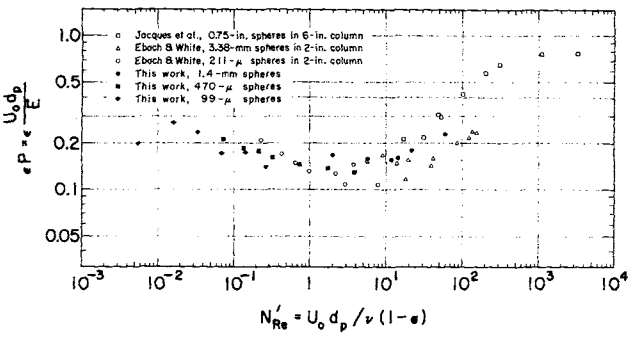

Fig. 4. Comparison with data of Jacques et al. and Ebach and White.

either particle diameter or the ratio of bed diameter to particle diameter. The possible weak decrease of Peclet number with particle diameter may well be within the calculational error due to assigning a nominal uniform particle diameter. Microscopic examination revealed that there was a range of bead sizes composing each set of microspheres as supplied by the manufacturer. Raimondi et al. (*19, 20*) report that the dispersion characteristics of a bed seem to be governed by the particle diameter corresponding to the 10% cumulative fraction.

DISCUSSION OF RESULTS

The ensuing discussion is an effort to correlate and interpret the available data on axial dispersion in packed beds. These data invariably cover large regions of packing where the effects of individual packing pieces and void spaces are well averaged out. Fundamental knowledge of flow and mixing patterns within the separate interstices of a bed is sparse. As a result any analysis of the mechanisms within voids and channels which control axial dispersion must be recognized as being to a large extent speculative.

A packed bed may be thought of as a series of main voids interconnected by smaller voids or channels so as to form a three-dimensional network. In a randomly packed bed these main voids are irregular in shape and are distributed about a certain effective size. When the main voids are well mixed and are interconnected by convective transport only, a mixing cell type of model may be applied to the system with the size and spacing of cells on the order of d_p. Although the main voids are larger than the interconnecting channels, they have a lower average velocity. As a result eddy or molecular diffusion should be able to cause appreciable mixing in the main voids without producing an amount of diffusion which is significant in comparison to the convective transport in the connecting channels. However, when diffuson in the channels is significant in relation to convection the picture of isolated well-mixed void cells must break down with a consequent decrease in Peclet number.

In the case of laminar flow and infinite Schmidt number fluid mixing can still be achieved, as suggested by Hennico et al. (*12*), when fluid filaments are forced together and are then split by geometry in such a way as to transfer some fluid from one filament to the other and thereby cause a velocity change for the transferred fluid. This mixing mechanism should give a Peclet group substantially smaller than would occur for well-mixed void cells, but should produce a Peclet number independent of Reynolds number.

The flow in packed beds for $N_{Re}' > 1{,}000$ is turbulent, with the result that the main voids should be well mixed. From Figure 4, ϵN_{Pe} is constant with respect to Reynolds number in this range as implied by a mixing cell model. If a single sequence of cells is postulated, the fact that ϵN_{Pe} is equal to 0.8 to 0.9 implies that the cell spacing in the axial direction is 2.5 ϵd_p.

The transition to laminar flow seems to take place over at least two decades of N_{Re}'. In this region behavior is dictated by the Schmidt number of the system. If N_{Sc} were infinite the only mixing mechanism after eddy diffusion damped out should be the filament mixing mentioned previously. The Peclet number would drop to a plateau characteristic of that mechanism and remain there for all smaller N_{Re}' greater than zero.

Dispersion in Gases

For low N_{Sc}, as the transition from fully turbulent to laminar flow begins, molecular diffusion apparently soon becomes strong enough in relation to throughput to aid the remaining eddies in keeping the main voids mixed. Such an effect can explain the small dip and rapid return of the data of McHenry and Wilhelm (*17*) to $\epsilon N_{Pe} =$ 0.8 to 0.9, as shown in Figure 5. At still lower Reynolds numbers axial diffusion in the channels between voids must break down the isolated mixing cells and eventually yield the behavior expected from dispersion governed solely by axial molecular diffusion. The gas phase data of Carberry and Bretton (*8*) were obtained for the dispersion of an air tracer in helium, for which $N_{Sc} = 1.7$. Their data are presented in Figure 5, with the Reynolds numbers recomputed on the basis of the viscosity of helium rather than air. It may be seen that the data agree well with an asymptotic expression (*13*), based on dispersion due to axial molecular diffusion alone with a tortuosity factor of $\sqrt{2}$ and a void fraction of 0.40:

$$\epsilon N_{Pe} = 0.85\, N_{Sc}\, N_{Re}' \qquad (8)$$

Equation (8) is represented by the dashed lines in Figure 5. Blackwell et al. (*4*) also found close agreement with Equation (8) for the dispersion of a helium tracer in argon.

The region of transition between axial molecular diffusion control and the isolated mixing cell model is covered by the data of Sinclair and Potter (*21*), who studied the dispersion of a mercury tracer in air, a system for which $N_{Sc} \simeq 1.2$. At high Reynolds numbers their results give ϵN_{Pe} constant at about 0.95, in agreement with the results of McHenry and Wilhelm. At lower Reynolds numbers the Peclet number falls off and seems to approach the axial molecular diffusion asymptote slowly. The beginning of the drop in Peclet number does not appear to be more than one decade in Reynolds number above the intersection of the axial-molecular-diffusion asymptote with the $\epsilon N_{Pe} = 0.95$ asymptote.

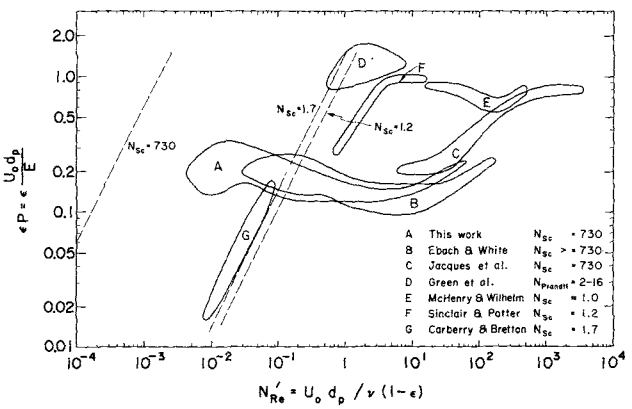

Fig. 5. Comparison of data for axial dispersion of mass and heat in gases and liquids.

Mass Dispersion in Liquids

The data for the present experiment were obtained for a system where $N_{Sc} = 730$. This value is calculated for 20°C. with a diffusivity based on the ionic mobilities of Harned and Owen (*11*). Because of the high Schmidt number it is logical to expect that ϵN_{Pe} will follow the hypothetical infinite Schmidt number curve for a greater range of N_{Re}' in the turbulent to laminar transition region than do the data for N_{Sc} near 1. This would account for the liquid phase data in Figure 5 being well below the gas phase data in the region $10 < N_{Re}' < 250$. At sufficiently low N_{Re}', radial mixing by diffusion within the main void cells should become important and can thus account for the increase in ϵN_{Pe} as N_{Re}' is further reduced below 10 for liquids in Figures 3, 4, and 5. However, for $N_{Sc} = 730$, the Reynolds number at which molecular diffusion becomes important is so low that there are probably few turbulent eddies, if any, remaining to interact with molecular diffusion and thus speed complete mixing in the main voids. As a result the return toward the extreme of well-mixed cells would be more gentle and further delayed with respect to the data for gas phase dispersion.

The nature and location of the rise in ϵN_{Pe} due to increasing mixing of the main voids by molecular diffusion can be interpreted in the following extremely oversimplified way:

In laminar flow a certain amount of mixing occurs from the geometric blending and splitting of fluid filaments which characterizes the lower limiting value of ϵN_{Pe} for $N_{Sc} \to \infty$. Any additional mixing within the main voids must occur through diffusional mass transfer between the various fluid streams entering a void cell. Figure 6(*a*) portrays two streams flowing into a common packing void and splitting apart again. Consider the effects on axial dispersion of radial mass transfer within a void space with short fluid contact times.

Let E_m be the efficiency of mixing in voids by diffusion over and above the geometrical stream blending and splitting of filaments in laminar flow. Then

$$\epsilon N_{Pe} = \epsilon N_{Pel} + E_m\,(\epsilon N_{Pet} - \epsilon N_{Pel}), \qquad (9)$$

where ϵN_{Pet} is the Peclet number for total mixing in void cells and ϵN_{Pel} is the Peclet number for infinite N_{Sc} in the laminar regime. The configuration shown in Figure 6(*a*) will be reduced to a cube of side δ, pictured in Figure 6(*b*), in order to derive the simplest possible model for a meaningful qualitative picture. The two entering streams are assumed to be of equal volume and velocity, and each enters the cell with a uniform concentration; however, the two streams have different concentrations from one another. The efficiency of mixing can be equated to the approach to equilibrium in the cell, and can thus be defined as

$$E_m = 1 - \frac{C_{ao} - C_{bo}}{C_{ai} - C_{bi}} = \frac{2(C_{ai} - C_{ao})}{C_{ai} - C_{bi}} \qquad (10)$$

Furthermore

$$C_{ai} - C_{ao} = \frac{K_L\,\delta(C_{ai} - C_{bi})}{u\,\delta/2} \qquad (11)$$

Therefore

$$E_m = \frac{4K_L}{u} \qquad (12)$$

Since the average individual mass transfer coefficient for either stream k_{Lm} will be twice K_L

$$E_m = \frac{2k_{Lm}}{u} \qquad (13)$$

The velocity of the imaginary interface between the two streams in the void cell is defined as $u_S = nu$. n will probably lie between 1 and 3, depending upon what velocity profile applies to the void cell and whether or not the interface falls at the point of maximum velocity. As long as $E_m < 0.5$, a penetration model should describe the mass transfer, yielding

$$k_{Lm} = 2\sqrt{\frac{Du_S}{\pi\delta}} \qquad (14)$$

It follows directly that

$$E_m = 4\sqrt{\frac{nD}{\pi u\delta}} \qquad (15)$$

and assuming $u = U_o/\epsilon$ and defining $\delta = d_p/m$, one obtains

$$E_m = 4\sqrt{\frac{nm}{\pi}}\left(\frac{D\epsilon}{U_o d_p}\right)^{1/2}$$

$$= 4\sqrt{\frac{nm\epsilon}{\pi(1-\epsilon)}}\,(N_{Sc})^{1/2}\,(N_{Re}')^{-1/2} \qquad (16)$$

If m is taken to be 1, n is taken to be 2, and $\epsilon = 0.4$, the multiplicative constant in Equation (16) will become 2.6. Applying Equation (16) to the system used in this experiment where $N_{Sc} = 730$ one obtains

$$E_m = 0.096\,(N_{Re}')^{-1/2} \qquad (17)$$

and

$$\epsilon N_{Pe} = \epsilon N_{Pel} + 0.096\,(N_{Re}')^{-1/2}\,(\epsilon N_{Pet} - \epsilon N_{Pel}) \qquad (18)$$

Figure 7 shows approximations for ϵN_{Pet} and ϵN_{Pel} along with the consequent curve of ϵN_{Pe} vs. N_{Re}' predicted by Equation (18). ϵN_{Pet} has been taken constant at 0.8 (curve 3) until N_{Re}' becomes low enough for axial molecular diffusion to become important. The transition (curve 5) of ϵN_{Pet} toward the asymptote of axial molecular diffusion control was obtained by taking the E involved in $\epsilon N_{Pe} = 0.8$ at any N_{Re}' to be additive with a superficial molecular diffusion contribution equal to $\epsilon D/\sqrt{2}$. ϵN_{Pel} (curve 2) follows the infinite Schmidt number curve during the transition from turbulent to laminar flow, and is assumed to line out at $\epsilon N_{Pel} = 0.06$ in the fully laminar region. The rise in ϵN_{Pe} due to Equation (18) is significant for $N_{Re}' < 10$ (curve 6). Above $\epsilon N_{Pe} = 0.4$ where $E_m > 0.5$ the penetration mass transfer model would break down and E_m should be lower than predicted by Equation (18). Curve 7 represents a reasonable transition between Equation (18) and the upper limit of ϵN_{Pet}.

Although the rise of ϵN_{Pe} due to Equation (18) is sharper than the rise of the observed data, it is apparent

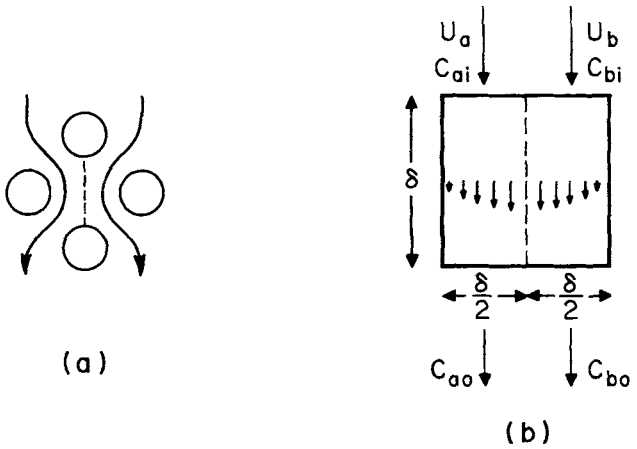

Fig. 6. Cell diffusion model.

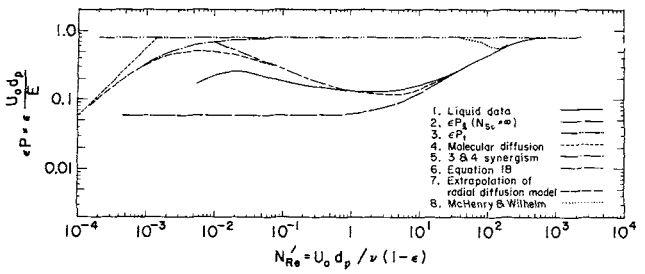

Fig. 7. Predicted effect of Schmidt or Prandtl number.

that Equation (18) provides a better representation of the rise than does the model of Taylor dispersion in a long capillary of uniform diameter. The capillary model requires a variation of ϵN_{Pe} with $(N_{Re}')^{-1}$ (*2, 13*) which is much steeper than the observed data and the prediction of Equation (18). For any reasonable values of n and m Equations (16) and (18) will succeed in locating the value of N_{Re}' at which the rise due to radial cell mixing begins, whereas a capillary model does not.

According to Equation (16) the gas phase data of McHenry and Wilhelm should not show an appreciable upward rise away from the infinite Schmidt number curve above $N_{Re}' = 30$. However, the return of ϵN_{Pe} toward the upper limit for well-mixed cells in this range of Reynolds numbers should be attributable to both eddy and molecular diffusion. A given amount of molecular diffusion could cause more mixing of individual void cells at low Schmidt numbers, because partial mixing by eddies would reduce the distances over which molecular diffusion must act. This explanation also suggests that the ϵN_{Pe} curve for $N_{Sc} = 730$ should be raised somewhat above the prediction of Equation (18) in the range $1 < N_{Re}' < 50$, as is shown by the actual data in Figure 7. To the extent that turbulence remains in the main void cells in this region, it will provide a synergistic effect with molecular diffusion for cell mixing.

The present data suggest that ϵN_{Pe} ceases to rise with decreasing Reynolds number and begins to fall again below $N_{Re}' = 0.01$. The maximum in ϵN_{Pe} seems to occur about one decade in N_{Re}' above the point at which it would be expected on the basis of the analysis leading to curve 7 in Figure 7. However, the assumption of direct additivity of the two dispersion coefficients used to generate curve 7 has no real physical justification.

Another factor should be considered. A certain amount of local fluid heating may have occurred in the present system in the vicinity of the two sets of electrodes. This heating could give rise to additional mixing by means of relatively large natural convection patterns. The effect would be to give a deceptively low value of ϵN_{Pe}, and the behavior would be most pronounced at the lower velocities. On the other hand, the results of Ebach and White (*9*) were obtained with a colorimetric technique and show the same leveling off and possible drop in ϵN_{Pe} at approximately the same N_{Re}' as in the present study. N_{Sc} for their system should have been still greater than in the present work.

For gas phase dispersion one would expect the same maximum ϵN_{Pe} (approximately 0.27) to occur before the drop due to axial molecular diffusion, if the diffusivity in the channels and voids is independent of position in the bed, and if ϵN_{Pet} is the same as at lower Reynolds numbers. However, the effective turbulent diffusivity may be greater in the larger voids than in the channels (greater maximum scale of turbulence) and, therefore, it is possible that the main voids could become well mixed while eddy diffusion in the channels is still unable to compete with convection. Since the values of ϵN_{Pe} found by Sinclair and Potter remain high to within one decade of the point of intersection of asymptotes at $N_{Re}' = 1$, this argument requires that some turbulence be present in the void spaces down to $N_{Re}' = 1$.

The differences between the maximum values of ϵN_{Pe} for gas and liquid systems could also be explained in another way. It is apparent that ϵN_{Pet} and/or ϵN_{Pel} could be changed in Figure 5 so as to provide a better fit of Equation (18) to the data of this study. A lowering of ϵN_{Pet} would be particularly effective for this purpose. It is possible that ϵN_{Pe} corresponding to fully mixed void cells in the laminar region could be lower than ϵN_{Pe} for fully mixed cells in the turbulent region. As has been pointed out by Perkins and Johnston (*19*) such behavior could result from the wider distribution of velocities in the connecting channels in laminar flow. Any realistic mixing cell model must take into account the fact that there is a three-dimensional network of cells and connecting channels. In a randomly packed bed it is reasonable to expect that there will be a range in sizes and configurations of void cells and connecting channels. As a consequence there is no reason to expect that the extreme of perfectly mixed cells will give the same concentration in all cells at a given horizontal bed level at a given time in a dynamic study. This distribution of velocities among the various connecting channels should be wider in laminar flow than in turbulent flow, since pressure drop varies with a lower power of velocity. As a consequence well-mixed cell concentrations at a given bed level should be less uniform in laminar flow than in turbulent flow, and ϵN_{Pet} could be lower in laminar flow than in turbulent flow.

The data of McHenry and Wilhelm and of Sinclair and Potter coupled with this argument would require that turbulence persist in the connecting channels down to $N_{Re}' = 1$; however, the conservation of mass suggests that the connecting channels would have a Reynolds number for flow that is higher than in the cells. As a result many channels might still be turbulent when most of the main cells have become laminar.

It should also be pointed out that the particular weighting factors of ϵ and $1 - \epsilon$ in ϵN_{Pe} and N_{Re}' suggested by Jacques et al. (*13*) have not been tested for liquids below $N_{Re}' = 10$ and for gases. However, the present data, the sphere data of Ebach and White, and the results of McHenry and Wilhelm, Carberry, and Bretton, and of Sinclair and Potter were all obtained for randomly packed spheres with ϵ very nearly equal to 0.4.

Dispersion of Heat in Liquids

Any model for the dispersion of mass at low concentrations in a flowing fluid should also be able to handle the dispersion of heat. Green, Perry, and Babcock (*10*) report data for axial dispersion of heat during liquid flow through a randomly packed bed of spheres. Their data for water and ethanol, covering a range of Prandtl numbers from 2 to 16, are shown in Figure 5. The computation of axial-dispersion coefficients for heat representing the fluid alone is complex and requires several corrections. Green et al. corrected their data for axial conduction in the solid packing and for convective heat transfer between the fluid and solid. On the other hand, as they have pointed out, no correction could be applied for any effect of radial conduction through the solid packing.

The Peclet numbers from Green et al. are in a range of N_{Re}' where some turbulence can still exist in the fluid and where eddy and molecular diffusion of heat should be able to keep the main voids well mixed; thus they should be high. The fact that ϵN_{Pe} is even higher than the values of 0.8 to 0.95 found for mass dispersion in gases

may be a symptom of an appreciable leveling out of temperature at a given bed level due to conduction through the packing. Such an effect would be important to the extent that cells at a given level do not have the same temperature at a given time, and its occurrence would lend some credence to the possibility of ϵN_{Pet} for mass dispersion in the laminar regime being less than ϵN_{Pet} in the turbulent regime. Both these values of ϵN_{Pet} would then be less than ϵN_{Pet} for heat dispersion with a large solid phase radial thermal conductivity.

Effect of Particle Size

The present data exhibit at most a weak effect of particle size on ϵN_{Pe} over a range of a factor of 28 in particle diameter. On this basis it does not seem likely that a particle-diameter effect can account for the difference in magnitude of ϵN_{Pe} in gas and liquid systems at the point where an effect due to axial molecular diffusion sets in, as has been suggested (*19*). Furthermore the gas phase studies of Sinclair and Potter (*22*) and of McHenry and Wilhelm (*17*) employed particle diameters similar to those employed in the present study and in the work of Ebach and White (*9*). The values of ϵN_{Pe} found by Jacques et al. (*13*) for liquids at low Reynolds numbers are in reasonable agreement in magnitude with the data of the present study for the same particle diameter, even though Jacques et al. employed a much larger bed diameter; hence there appears to be no important effect of d_t/d_p.

ACKNOWLEDGMENT

The authors are grateful for the constant interest and frequent helpful advice of Professor Theodore Vermeulen. This work was performed in the Lawrence Radiation Laboratory under the auspices of the U.S. Atomic Energy Commission.

NOTATION

a = amplitude of the breakthrough curve (recorder units)
C = concentration
D = molecular diffusivity
d_p = particle diameter
d_t = column diameter
E = axial dispersion coefficient based on the open bed ($\epsilon E'$)
E' = mean linear interstitial dispersion coefficient
E_M = efficiency of mixing in voids over filament mixing
h = elapsed recorder chart distance between an initial perfect step and the midpoint of the breakthrough
Δh = recorder chart distance between breakthroughs 1 and 2
K_L = overall mass transfer coefficient
k_{Lm} = average mass transfer coefficient for either stream
L = distance between conductivity cells
m = constant, d_p/δ
n = constant, u_s/u
N_{Pe} = packing Peclet number, $U_o d_p/E$, Ud_p/E'
N_{Pe}' = column Peclet number, LU_o/E
N_{Pel} = Peclet number for infinite N_{Sc} in the laminar regime
N_{Pet} = Peclet number for total void mixing
N_{Re} = Reynolds number, $U_o d_p/\nu$
N_{Re}' = modified Reynolds number, $U_o d_p/\nu(1 - \epsilon)$
N_{Sc} = Schmidt number, ν/D
S = dimensionless midpoint slope = $(h \tan \theta)/a$
$\tan \theta$ = midpoint slope of the breakthrough curve (recorder units)
U = interstitial velocity
U_o = superficial velocity
u = average velocity
u_s = interfacial velocity (nu)
X = recorder chart speed

Greek Letters

δ = length of cell side
ϵ = void fraction
λ = inhomogeneity factor
ν = kinematic viscosity

Subscripts

1 = upstream breakthrough point
2 = downstream breakthrough point
i = entering
o = exiting
a = stream a
b = stream b

LITERATURE CITED

1. Ampilogov, I. E., A. N. Kharim, and I. S. Kurochkina, *Zh. Fiz. Khim.*, **32**, 141 (1958).
2. Aris, Rutherford, *Proc. Roy. Soc.* (*London*), **A235**, 67 (1956).
3. Beran, M. J., Ph.D. thesis, Harvard Univ. (1955).
4. Blackwell, R. J., J. R. Rayne, and W. M. Terry, *Trans. Am. Inst. Mech. Engrs.*, **216**, 1 (1959).
5. Blackwell, R. J., *Soc. Petrol. Engrs. J.*, **2**, 1 (1962).
6. Brigham, W. E., P. W. Reed, and J. N. Dew, *ibid.*, **1**, 1 (1961).
7. Cairns, E. J., and J. M. Prausnitz, *Chem. Eng. Sci.*, **12**, 20 (1960).
8. Carberry, J. J., and R. H. Bretton, *A.I.Ch.E. J.*, **4**, 367 (1958).
9. Ebach, E. A., and R. R. White, *ibid.*, 161.
10. Green, D. W., R. H. Perry, and R. E. Babcock, *ibid.*, **10**, 645 (1964).
11. Harned, H. S., and B. B. Owen, "The Physical Chemistry of Electrolytic Solutions," Reinhold, New York (1958).
12. Hennico, A., G. L. Jacques, and Theodore Vermeulen, *Lawrence Radiation Lab. Rept. UCRL-10696*, Pt. I (1964); *Chem. Eng. Sci.*, in press.
13. Jacques, G. L., A. Hennico, J. S. Moon, and Theodore Vermeulen, *Lawrence Radiation Lab. Rept. UCRL-10696*, Pt. II (1964); *Chem. Eng. Sci.*, in press.
14. Klinkenberg, A., and E. Sjenitzer, *Chem. Eng. Sci.*, **5**, 258 (1956).
15. Klinkenberg, A., *Trans. Inst. Chem. Engrs.*, **43**, T141 (1965).
16. Liles, A. W., and C. J. Geankoplis, *A.I.Ch.E. J.*, **6**, 591 (1960).
17. McHenry, K. W., Jr., and R. H. Wilhelm, *ibid.*, **3**, 83 (1957).
18. Miller, S. F., and C. J. King, *Lawrence Radiation Lab. Rept. UCRL-11951* (1965).
19. Perkins, T. K., and O. C. Johnston, *Soc. Petrol. Engrs. J.*, **3**, 70 (1963).
20. Raimondi, P., G. H. F. Gardner, and C. B. Petrick, paper presented at A.I.Ch.E. San Francisco Meeting (December, 1959).
21. Rifai, M. N. E., Ph.D. thesis, Univ. California, Berkeley (1956).
22. Sinclair, R. J., and O. E. Potter, *Trans. Inst. Chem. Engrs.*, **43**, T3 (1965).
23. Stahel, E. P., and C. J. Geankoplis, *A.I.Ch.E. J.*, **10**, 174 (1964).
24. Strang, D. A., and C. J. Geankoplis, *Ind. Eng. Chem.*, **50**, 1305 (1958).
25. Tompkins, E. R., D. H. Harris, and J. X. Khym, *Rept. AECD-2128*, Oak Ridge, Tenn. (1948); *J. Am. Chem. Soc.*, **71**, 2504 (1949).
26. Vermeulen, Theodore, and N. K. Hiester, *Ind. Eng. Chem.*, **44**, 636 (1952).
27. von Rosenberg, D. U., *A.I.Ch.E. J.*, **2**, 55 (1956).

Manuscript received August 10, 1965; revision received January 31, 1966; paper accepted February 15, 1966.